

## Adsorption of Cu(II)-EDTA chelates on amino-functionalized mesoporous manganese dioxide from acid wastewater

Jie Yu<sup>a</sup>, Xue Shi<sup>a</sup>, Yili Wang<sup>a,b</sup>, Hongjie Wang<sup>a, b,\*</sup>

<sup>a</sup>College of Environmental Science and Engineering, Beijing Forestry University, Beijing 100083, China, Tel./Fax: +86 10 6233 6900; email: 1224501152@qq.com, whj\_99@hotmail.com (H. Wang)

<sup>b</sup>Beijing Key Lab for Source Control Technology of Water Pollution, Beijing 100083, China Tel./Fax: +86 10 6233 6900; email: wanyilimail@126.com (Y. Wang)

Received 23 January 2016; Accepted 11 July 2016

### ABSTRACT

To eliminate the pollution of high stable metal-ethylenediaminetetraacetic acid (EDTA) complexes, manganese dioxide ( $\delta$ -MnO<sub>2</sub>) and amino-functionalized mesoporous manganese dioxide (NH<sub>2</sub>-MnO<sub>2</sub>) were used as adsorbents for removing Cu(II)-EDTA chelates from acid wastewater. The removal efficiency of the chelates by both adsorbents decreased markedly with the solution pH varying from 3.5 to 8.0. Higher ionic strength had obviously negative effect on the capture of the chelates. Langmuir model could describe well the adsorption process of Cu(II)-EDTA chelates onto both adsorbents, and the maximum adsorption capacity of NH<sub>2</sub>-MnO<sub>2</sub> was over two times higher than that of the un-functionalized  $\delta$ -MnO<sub>2</sub>. The equilibrium could be achieved in 1 h, and the pseudo-first-order equation fitted well for the adsorption process. The uptake of Cu(II)-EDTA chelates onto NH<sub>2</sub>-MnO<sub>2</sub> took place on the external surface of the adsorbent. The electrostatic interaction between amino groups on the adsorbent and carboxyl groups of Cu(II)-EDTA dominated the adsorption process.

*Keywords:* Adsorption; Amino-functionalization; Cu(II)-EDTA chelates; Manganese dioxide

### 1. Introduction

As one of the most widely used sequesters, the ethylenediaminetetraacetic acid (EDTA) can combine with heavy metal ions and promote them into absolutely stable metal-EDTA complexes, such as Pb(II)-EDTA, Co(II)-EDTA, Cu(II)-EDTA, and so on. In view of the nature of the high solubility, low-level biodegradability and excellent stability of the metal-EDTA complexes, various processes, such as chelating precipitation [1], catalytic oxidation [2], ion exchange [3], adsorption, micro-electrolysis [4] and so on, have been set up to eliminate the potential menace of the discharge of the complexes. Among these methods, adsorption process, due to its great virtue of efficiency, flexibility, easy operation and good selectivity [5], is one of the most widespread and effective methods for the removal of metal complexes. Poly-

hydroxyl Fe/Zr pillared montmorillonite [6] and polyurethane modified with dithiocarbamate [7] had been utilized for the capture of Cu(II)-EDTA complexes from wastewater and performed effectively. Agent derived from carbon disulfide and hydrazine hydrate could sequester Cu(II)-EDTA chelates spontaneously and exothermically in acid condition with high initial copper concentration [8]. Activated carbon, goethite, silica, iron hydroxides and TiO<sub>2</sub> and so on were also extensively used and performed well [9–14]. However, most of these adsorbents had their shortcomings of low removal efficiency and long equilibrium. Thus, it is still imperative to develop higher effective adsorbents to remove metal-EDTA complexes. One of the efficient ways is to graft functional organic groups, including amino, allylamine and pyrimidine groups and so on, onto traditional adsorbents for the sake of attaining greater adsorption capacity [15–17]. Especially, amino-functionalized mesoporous silica [18,19] and amino-functionalized mesoporous manganese dioxide (NH<sub>2</sub>-MnO<sub>2</sub>) [20] had been developed for excellent adsorp-

\*Corresponding author.

Presented at the 6th IWA-ASPIRE Conference & Exhibition, Beijing, China, 20–24 September 2015.

tion ability for heavy metal ions as well as high adsorption capacity for toxic anions [21,22]. However, the uptake mechanism of the metal ions and the coexisting chelating agents by the amino-functionalized materials in aqueous solution needed to be further explored.

In the current study, the adsorption behaviors of Cu(II)-EDTA chelates from acid wastewater on manganese dioxide ( $\delta$ -MnO<sub>2</sub>), the surface characteristics of sorbent and sorption mechanisms were elucidated through Fourier transform infrared spectroscopy (FTIR) and X-ray photoelectron spectroscopy (XPS) analysis.

## 2. Materials and methods

### 2.1. Materials

All chemicals, such as copper nitrate (Cu(NO<sub>3</sub>)<sub>2</sub>·5H<sub>2</sub>O), ethylenediaminetetraacetic acid disodium (Na<sub>2</sub>EDTA), hydrogen peroxide (H<sub>2</sub>O<sub>2</sub>), potassium permanganate (KMnO<sub>4</sub>), sodium hydroxide (NaOH), hydrogen nitrate (HNO<sub>3</sub>), toluene, acetone and ethanol, were analytical grade and purchased from Beijing Chemical Co. (Beijing, China). (3-aminopropyl) trimethoxysilane (APTMS) was purchased from Alfa Aesar Co. (Ward Hill, MA, USA). The Cu(II) stock solutions were prepared by dissolving Cu(NO<sub>3</sub>)<sub>2</sub>·5H<sub>2</sub>O in appropriate amounts of deionized water. The concentrations of Cu(II) were always given as elemental copper concentration. All chemicals were used directly without further purification.

### 2.2. Adsorbent preparation

The NH<sub>2</sub>-MnO<sub>2</sub> was prepared according to previous work [20], which was conducted as following procedure: 1 g of  $\delta$ -MnO<sub>2</sub> was reacted with 1 mL of APTMS in toluene under nitrogen atmosphere with refluxed condition and violent agitation for 12 h. The suspension was filtered and washed by toluene, acetone and ethanol, and then the cake was dried at 105°C for 6 h to obtain the amino-functionalized mesoporous adsorbent.

### 2.3. Characterization

The freeze-dried samples of  $\delta$ -MnO<sub>2</sub> and NH<sub>2</sub>-MnO<sub>2</sub> were characterized using several characterization techniques. The N<sub>2</sub> adsorption/desorption isotherms of the adsorbents were described using a NOVA 1200 BET analyzer (ASAP 2000, Micromeritics Co. USA) with the samples degassed at 150°C and 105 Torr under vacuum for at least 6 h. The virgin and the reacted adsorbents were analyzed by FTIR spectroscopy (Vertex 70, Bruker Optics, France). Each sample was mixed with pure potassium bromide which acted as background at an approximate mass ratio of 1:100 (sample:KBr) and then grounded in an agate mortar. The resulting mixture was pressed at 13 tons for 2 min to form a pellet which was characterized using FTIR spectrophotometer using a transmission model. The XPS (Kratos AXIS Ultra, UK) spectra were obtained by applying the aluminum anode X-ray source with a monochromator (Al K $\alpha$ ,  $h\nu = 1,486.71$  eV) operated at 15 kV and 15 mA. All binding energy values were determined with respect to C 1 s line (284.6 eV) originating from adventitious

carbon. The XPS results were collected in binding energy forms and fitted using the software of Vision (PR2.1.3) and Casa XPS (2.3.12Dev7).

### 2.4. Batch adsorption experiments

The adsorption isotherm experiments were performed in Cu(II)-EDTA solutions at 25°C. The solutions were prepared by dissolving equimolar of Cu(NO<sub>3</sub>)<sub>2</sub>·5H<sub>2</sub>O and Na<sub>2</sub>EDTA in deionized water for 24 h. The initial copper concentrations were 0.05, 0.1, 0.15, 0.2, 0.4, 0.6, 0.8 and 1.0 mmol L<sup>-1</sup>. The ionic strength was maintained as 0.01 mol L<sup>-1</sup> NaNO<sub>3</sub>, and the solution pH was controlled at 3.5 ± 0.2. After that, NH<sub>2</sub>-MnO<sub>2</sub> or  $\delta$ -MnO<sub>2</sub> was added into the solutions and reacted for 12 h with shaking speed of 170 rpm.

The adsorption kinetics experiments were carried out at 25°C, and Cu(II)-EDTA solution with initial copper concentration 0.1 mmol L<sup>-1</sup> was added in a conical flask. The ionic strength was 0.01 mol L<sup>-1</sup> NaNO<sub>3</sub>, and the solution pH was adjusted to 3.5 ± 0.2. Then NH<sub>2</sub>-MnO<sub>2</sub> or  $\delta$ -MnO<sub>2</sub> was added to the solution to get suspensions with shaking speed of 170 rpm. The samples were taken from the suspensions at various time intervals (2 min to 24 h).

Experiments of the effect of different solution pH and ionic strength were performed in solutions with equimolar ratio of Cu(II) and EDTA at 25°C; the initial concentration of Cu(II)-EDTA was 0.1 mmol L<sup>-1</sup>. The solution pH ranged from 3.5 to 8 and used 0.01, 0.05 and 0.1 mol L<sup>-1</sup> NaNO<sub>3</sub> as background electrolyte. The solution pH was adjusted to corresponding value with 0.1 mol L<sup>-1</sup> HNO<sub>3</sub> or 0.1 mol L<sup>-1</sup> NaOH. The suspensions were shaken with a speed of 170 rpm and reacted for 12 h.

All the samples collected above were filtered by a 0.45  $\mu$ m filter membrane, and the residual copper concentrations were determined by atomic absorption spectrophotometer (AAS, AA-6300 Shimadzu Co., Japan).

The uptake of Cu(II) at time  $t$  ( $q_t$ ) was calculated using the following equation:

$$q_t = \frac{V(C_0 - C_t)}{W} \quad (1)$$

where  $C_0$  (mg L<sup>-1</sup>) is the initial concentration of Cu(II) in solution;  $C_t$  (mg L<sup>-1</sup>) is the concentration of Cu(II) in solution at time  $t$ ;  $W$  (g) is the weight of adsorbent and  $V$  (L) is the volume of the solution.

### 2.5. Modeling of adsorption isotherm and kinetics

The adsorption isotherm experimental results were fitted for using Langmuir (Eq. (2)) and Freundlich isotherm models (Eq. (3)), respectively.

$$q_e = \frac{q_{max} K_L C_e}{1 + K_L C_e} \quad (2)$$

$$q_e = K_f C_e^{1/n} \quad (3)$$

where  $q_e$  is the equilibrium amount of Cu(II) adsorbed on adsorbent (mg g<sup>-1</sup>);  $q_{max}$  is the maximum amount of Cu(II) adsorbed (mg g<sup>-1</sup>);  $C_e$  is the equilibrium concentration of

Cu(II) ( $\text{mg L}^{-1}$ );  $K_L$  is the Langmuir adsorption constant ( $\text{L mg}^{-1}$ );  $K_F$ ,  $((\text{mg g}^{-1})(\text{L mg}^{-1})^{1/n})$  and  $n$  are the Freundlich adsorption isotherm constants.

The thermodynamic parameters of the adsorption process including Gibbs free energy ( $\Delta G$ ), enthalpy ( $\Delta H$ ) and entropy ( $\Delta S$ ) were also calculated according to the following equations:

$$\Delta G = -RT \ln \left( \frac{q_e}{C_e} \right) \quad (4)$$

$$\Delta G = \Delta H - T\Delta S \quad (5)$$

$$\ln \left( \frac{q_e}{C_e} \right) = \frac{\Delta S}{R} - \frac{\Delta H}{RT} \quad (6)$$

where  $R$  is gas constant ( $8.314 \text{ J (K}^{-1}\cdot\text{mol}^{-1})$ ), and  $T$  (K) is the temperature.

The pseudo-first-order kinetic model (Eq. (7)) and pseudo-second-order equation (Eq. (8)) were represented by the Lagergren equation as given below:

$$\log(q_e - q_t) = \log(q_e) - \frac{K_1 t}{2.303} \quad (7)$$

$$\frac{t}{q_t} = \frac{1}{K_2 q_e^2} + \frac{t}{q_e} \quad (8)$$

where  $K_1$  and  $K_2$  ( $\text{g (mg}^{-1} \text{ min}^{-1})$ ) are the rate constants of pseudo-one-order and second-order equation, respectively;  $q_t$  is the same as Eq. (1) and  $t$  is the time (h).

### 3. Results and discussion

#### 3.1. Effect of pH and ionic strength

As depicted in Fig. 1, the solution pH had great influence on the uptake of the Cu(II)-EDTA chelates by both adsorbents. Contrasting to the results of the blank Cu(II)

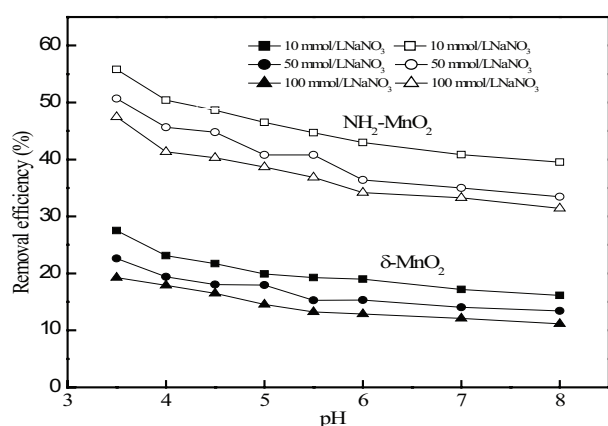


Fig. 1. Effect of pH and ionic strength on removal efficiency of Cu(II)-EDTA.  
Note: Cu:EDTA = 1:1,  $C_{0,Cu} = 0.1 \text{ mmol L}^{-1}$ , dosage =  $1.0 \text{ g L}^{-1}$ ,  $T = 25 \pm 1^\circ\text{C}$ .

solutions [20], the removal efficiency of the Cu(II)-EDTA chelates by both adsorbents decreased markedly with the solution pH varying from 3.5 to 8.0. The removal efficiency of NH<sub>2</sub>-MnO<sub>2</sub> was much higher than that of δ-MnO<sub>2</sub> at corresponding situations. According to the calculated results by Visual MINTEQ (3.0), the dominating copper species in solutions with equimolar ratio of Cu(II) and EDTA were CuHEDTA<sup>-</sup> anions and CuEDTA<sup>2-</sup> anions in the pH range from 3 to 10, while the copper ions rarely existed in the solutions because of the excellent chelating ability of EDTA. Moreover, the point of zero charge ( $\text{pH}_{\text{PZC}}$ ) of NH<sub>2</sub>-MnO<sub>2</sub> was around 4.3. When the solution  $\text{pH} < \text{pH}_{\text{PZC}}$ , the protonation of amino groups resulted in the electrostatic interaction with the negatively charged Cu(II)-EDTA anions. When the solution  $\text{pH} > \text{pH}_{\text{PZC}}$ , the deprotonation of amino groups would make negative effect on attachment of Cu(II)-EDTA complexes by electrostatic interaction.

On the other side, with the ionic strength increasing from 0.01 to 0.1 mol L<sup>-1</sup> of NaNO<sub>3</sub>, a significant decrease of Cu(II)-EDTA chelates uptake by NH<sub>2</sub>-MnO<sub>2</sub> or δ-MnO<sub>2</sub> was detected, which indicated the formation of outer-sphere complexation dominating the adsorption process during the pH range [23].

#### 3.2. Adsorption isotherms and thermodynamics

The adsorption isotherms of NH<sub>2</sub>-MnO<sub>2</sub> and δ-MnO<sub>2</sub> for Cu(II)-EDTA chelates were described in Fig. 2. Both of the isotherms showed the same trend, while the NH<sub>2</sub>-MnO<sub>2</sub> displayed much higher adsorption capacity for Cu(II)-EDTA chelates than that of δ-MnO<sub>2</sub> at corresponding conditions. To further examine the correlation between the adsorbed and the residual Cu(II)-EDTA chelates, Langmuir model and Freundlich model were introduced to describe the adsorption process. The values of coefficient of determination indicated that the Langmuir model ( $R^2 = 0.987$ ) gave a better fit for the experimental data. The  $q_{\text{max}}$  calculated by Langmuir model was consistent with the experimental equilibrium

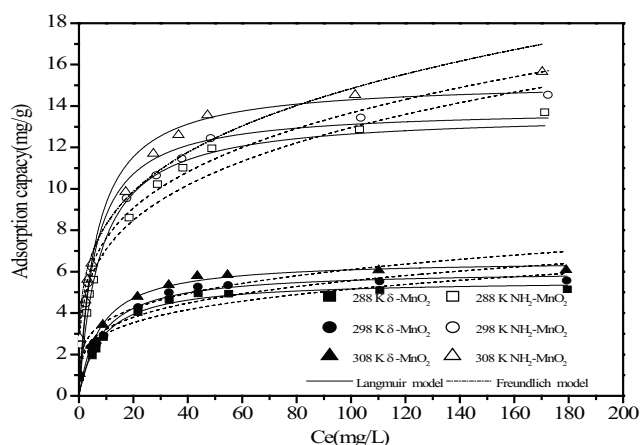


Fig. 2. Adsorption isotherms of Cu-EDTA at different temperatures.  
Note: Cu:EDTA = 1:1, dosage =  $1.0 \text{ g L}^{-1}$ ,  $\text{pH} = 3.5$ ,  $0.01 \text{ mol L}^{-1} \text{ NaNO}_3$ ,  $T = 25 \pm 1^\circ\text{C}$ .

Table 1  
Comparison of the  $q_{max}$  of various adsorbents

Adsorbent	pH	$q_{max}$ (mg g <sup>-1</sup> )	Reference
Fe/Zr pillared montmorillonite	6.0	16.67	[6]
Active carbon	3.1	2.88	[9]
Fe(OH) <sub>3</sub>	11	33	[12]
NNN-SBA-15	5.5	26.3	[17]
$\delta$ -MnO <sub>2</sub>	3.5	5.65	This work
NH <sub>2</sub> -MnO <sub>2</sub>	3.5	14.45	This work

adsorption capacity ( $q_{exp}$ ). And the comparison of the adsorption capacity of different sorbent was listed in Table 1. On the basis of the hypotheses of Langmuir isotherm model, the adsorption of Cu(II)-EDTA by these adsorbents was inferred to monolayer sorption. Meanwhile, the negative value of  $\Delta G$  and the positive values of  $\Delta H$  and  $\Delta S$  determined a spontaneous and endothermic adsorption process.

### 3.3. Adsorption kinetics and activation energy

To investigate the relationship between adsorption capacity of NH<sub>2</sub>-MnO<sub>2</sub> or  $\delta$ -MnO<sub>2</sub> for Cu(II)-EDTA chelates and contacting time, the adsorption kinetics experiments were conducted, and the results were presented in Fig. 3. The equilibrium was achieved in short time, and the uptake of Cu(II)-EDTA chelates was remarkably enhanced by the amino functionalization process. Both of the curves showed almost the same trend, which indicated the possibly similar adsorption mechanism of Cu(II)-EDTA by two adsorbents at corresponding time. Both of the pseudo-first-order and pseudo-second-order equations could fit well for the adsorption behavior of Cu(II)-EDTA chelates on the adsorbents, while the pseudo-first-order equation obtained a more realistic value of equilibrium capacity. This indicated that the adsorption process of Cu(II)-EDTA chelates was dominated by physisorption process.

Meanwhile, the temperature had obvious positive effect on the uptake of Cu(II)-EDTA chelates. Arrhenius equation parameters were fitted by the rate constants simulated in pseudo-first-order kinetics to determine temperature independent rate parameters and adsorption type. The values of the calculated activation energy ( $E_a$ ) for Cu(II)-EDTA chelates adsorption onto NH<sub>2</sub>-MnO<sub>2</sub> and  $\delta$ -MnO<sub>2</sub> were 11.78 and 12.21 kJ mol<sup>-1</sup>, which demonstrated that physisorption process dominated the adsorption process.

### 3.4. BET

The nitrogen adsorption/desorption isotherms of the virgin and Cu(II)-EDTA saturated NH<sub>2</sub>-MnO<sub>2</sub> were shown in Fig. 4. Both of the curves could be ascribed to

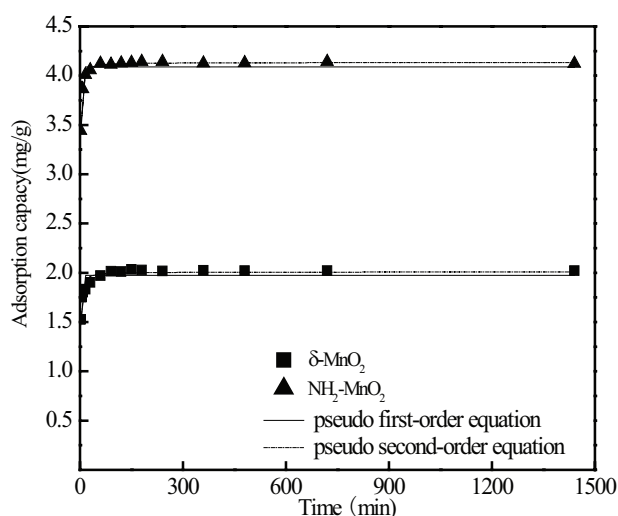


Fig. 3. Adsorption kinetics of Cu-EDTA on  $\delta$ -MnO<sub>2</sub> and NH<sub>2</sub>-MnO<sub>2</sub>.  
Note: Cu:EDTA = 1:1,  $C_{0,Cu}$  = 0.01 mmol L<sup>-1</sup>, dosage = 1.0 g L<sup>-1</sup>, pH = 3.5, 0.01 mol L<sup>-1</sup> NaNO<sub>3</sub>.

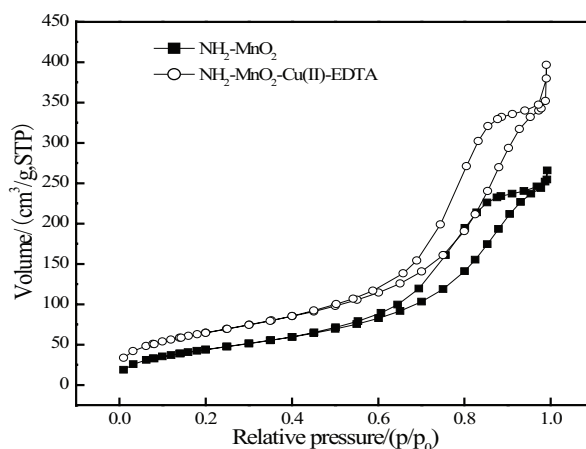


Fig. 4. Nitrogen sorption/desorption isotherms before and after adsorption of Cu(II)-EDTA chelates onto  $\delta$ -MnO<sub>2</sub> and NH<sub>2</sub>-MnO<sub>2</sub>.

the type IV isotherms classified by International Union of Pure and Applied Chemistry (IUPAC), and the isotherms showed obvious nitrogen hysteric loops at  $\sim 0.5\text{--}0.9 P/P_0$ , typical of the nitrogen filling of mesopores. Parameters of the surface structure (Table 2) showed that the specific surface area of NH<sub>2</sub>-MnO<sub>2</sub> was much less than that of the un-functionalized one. Comparing to the  $t$ -plot results of  $\delta$ -MnO<sub>2</sub> and NH<sub>2</sub>-MnO<sub>2</sub>, the change was mainly ascribed to the decrease of the external surface area. Meanwhile, both of the specific surface area and the external surface area of the Cu(II)-EDTA loaded  $\delta$ -MnO<sub>2</sub> and NH<sub>2</sub>-MnO<sub>2</sub> increased obviously. It indicated that the chelates were anchored on the external surface of  $\delta$ -MnO<sub>2</sub> and NH<sub>2</sub>-MnO<sub>2</sub>.

Table 2  
BET characterization of  $\delta$ -MnO<sub>2</sub> and NH<sub>2</sub>-MnO<sub>2</sub> before and after adsorption.

	BET surface area (m <sup>2</sup> g <sup>-1</sup> )	<i>t</i> -plot micropore area (m <sup>2</sup> g <sup>-1</sup> )	<i>t</i> -plot external surface area (m <sup>2</sup> g <sup>-1</sup> )	Pore volume (cm <sup>3</sup> g <sup>-1</sup> )	Pore size (nm)
MnO <sub>2</sub>	274.77	44.45	230.32	0.62	9.98
MnO <sub>2</sub> -Cu(II)-EDTA	271.31	22.26	249.05	0.64	10.15
NH <sub>2</sub> -MnO <sub>2</sub>	164.78	39.62	125.16	0.41	9.05
NH <sub>2</sub> -MnO <sub>2</sub> -Cu(II)-EDTA	228.61	24.15	204.46	0.33	8.65

### 3.5. FTIR

The FTIR spectra of NH<sub>2</sub>-MnO<sub>2</sub> before and after Cu(II)-EDTA uptake were presented in Fig. 5. The intensity enhancement of the peaks at 2,854 and 2,926 cm<sup>-1</sup> were attributed to C-H stretching and bending vibrations in CH<sub>2</sub> groups, and the appearance of the stretching vibration of carboxyl groups (C=O) at 1,738 cm<sup>-1</sup> demonstrated the uptake of Cu(II)-EDTA. After adsorption, the band of O-H stretching vibration of the surface hydroxyl groups was red-shifted to 3,439 cm<sup>-1</sup> and strengthened obviously, which could be ascribed to the formation of strong hydrogen bond. The appearance of the broad band at 2,031 cm<sup>-1</sup> was ascribed to the interaction of protonated amino groups (-NH<sub>3</sub><sup>+</sup>) of NH<sub>2</sub>-MnO<sub>2</sub> and carboxyl groups of Cu(II)-EDTA. Meanwhile, the asymmetric variable angle vibration of -NH<sub>3</sub><sup>+</sup> at 1,469 cm<sup>-1</sup> was obviously decreased, which further demonstrated the -NH<sub>3</sub><sup>+</sup> of NH<sub>2</sub>-MnO<sub>2</sub> accounting for the uptake of Cu(II)-EDTA.

### 3.6. XPS

To examine the chemical environment of the adsorbent before and after adsorption and to clarify the adsorption mechanism for Cu(II)-EDTA captured by NH<sub>2</sub>-MnO<sub>2</sub>, XPS spectrum was conducted. The wide-scanned XPS spectra (not provided) over a binding energy from 0 to 1,100 eV showed clear Cu 2p binding energy peak about 934–935 eV after adsorption, which demonstrated the uptake of the copper species by NH<sub>2</sub>-MnO<sub>2</sub>.

Detail spectra of the peaks for C 1 s, O 1 s and N 1 s were shown in Figs. 6–8. The peaks of C 1 s in Fig. 6 before adsorption were observed at 284.9, 286.4 and 287.8 eV, which were assigned to Si-C, C-C/C-H and C-N, respectively [24]. After adsorption of the pollutants, a new peak at 288.8 eV ascribed to O=C-O appeared, which indicated the uptake of the EDTA on the surface of NH<sub>2</sub>-MnO<sub>2</sub>.

The peak of O 1 s before interaction in Fig. 7 could be attributed to a sum of three peaks. The peaks of binding energy at 530.0 and 531.8 eV were assigned to the lattice oxygen, which existed in manganese oxides [25]. Another peak of binding energy at 533.2 eV attributed to the surface adsorbed oxygen [26]. After adsorption, these peaks shifted slightly and generated a new peak at 533.3 eV, which ascribed to C=O [27]. Considering of the main species of the pollutants in the solutions, the uptake of the Cu(II)-EDTA chelates was confirmed.

The peak of lower binding energy of N 1 s at 400.0 eV in Fig. 8 could be assigned to -NH-/-NH<sub>2</sub>, while the other one of binding energy at 401.1 eV could be assigned to -

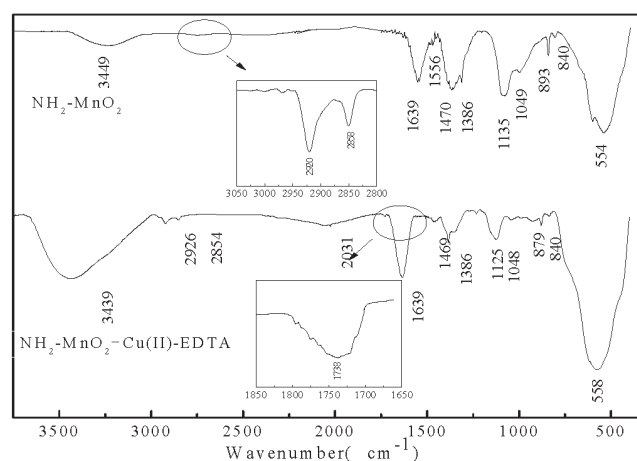


Fig. 5. The FTIR spectra of NH<sub>2</sub>-MnO<sub>2</sub> before and after adsorption.

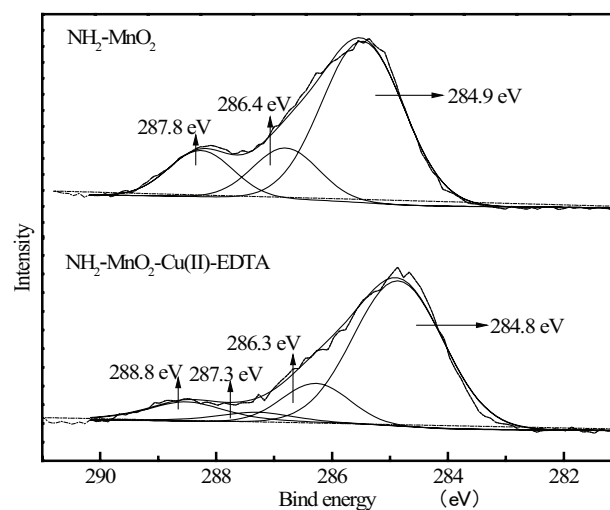


Fig. 6. XPS detailed spectra of NH<sub>2</sub>-MnO<sub>2</sub> with C 1 s before and after adsorption.

NH<sub>3</sub><sup>+</sup> [28]. The peak of -NH<sub>3</sub><sup>+</sup> shifted toward higher binding energy after the capture of Cu(II)-EDTA, which indicated the electrostatic interaction between negatively charged Cu-EDTA anions and positively charged protonated amino groups on the adsorbent [19].

In general, the changes of binding energy of C 1 s, O 1 s and N 1 s, especially the clear increase of the proportion of -NH<sub>3</sub><sup>+</sup> after uptake of Cu(II)-EDTA chelates, indicated the

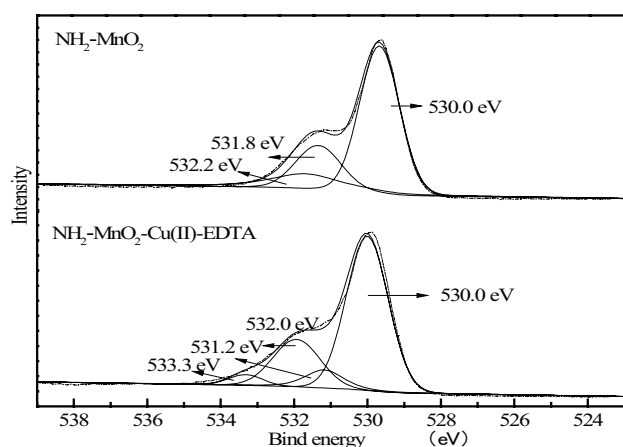


Fig. 7. XPS detailed spectra of  $\text{NH}_2\text{-MnO}_2$  with O 1s before and after adsorption.

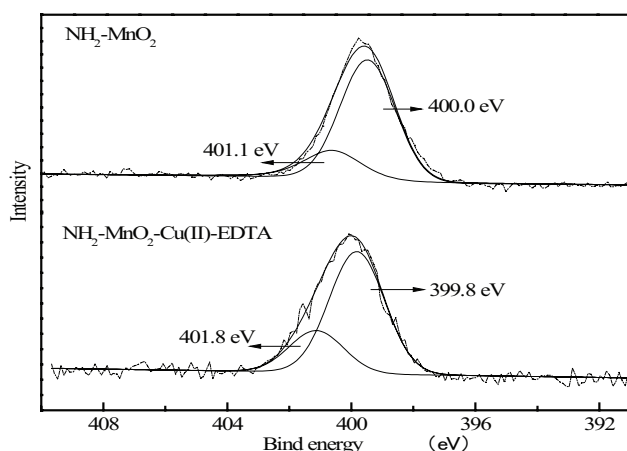


Fig. 8. XPS detailed spectra of  $\text{NH}_2\text{-MnO}_2$  with N 1s before and after adsorption.

interaction of amino groups on the surface of  $\text{NH}_2\text{-MnO}_2$  and the carboxyl groups of  $\text{Cu(II)-EDTA}$  chelates rather than the copper ions.

#### 4. Conclusions

$\text{NH}_2\text{-MnO}_2$  had a stronger ability to uptake  $\text{Cu(II)-EDTA}$  chelates from aqueous solutions than that of the un-functionalized  $\delta\text{-MnO}_2$ . Lower solution pH and ionic strength were benefits for the uptake of the chelates. The Langmuir model fitted well for the experimental data, and the maximum adsorption capacity of  $\text{Cu(II)-EDTA}$  chelates on  $\text{NH}_2\text{-MnO}_2$  was two times more than that of the un-functionalized one. The values of the calculated activation energy ( $E_a$ ) demonstrated physisorption process dominating the adsorption process. The interaction of  $\text{Cu(II)-EDTA}$  chelates and  $\text{NH}_2\text{-MnO}_2$  mainly occurred on the external surface of the adsorbent. The adsorption of  $\text{Cu(II)-EDTA}$  chelates onto  $\text{NH}_2\text{-MnO}_2$  attributed to the electrostatic inter-

action between positively charged amino groups ( $-\text{NH}_3^+$ ) on the adsorbent and the negatively charged  $\text{Cu(II)-EDTA}$  anions. The carboxyl groups rather than the copper ions of  $\text{Cu(II)-EDTA}$  chelates accounted for the interactions with  $\text{NH}_2\text{-MnO}_2$ .

#### Acknowledgments

This work was supported by Major Science and Technology Program for Water Pollution Control and Treatment (2015ZX07204-002) and the National Natural Science Research Fund (Nos. 51578067 and 51278051).

#### References

- [1] N.P. Hankins, N. Lu, N. Hilal, Enhanced removal of heavy metal ions bound to humic acid by polyelectrolyte flocculation, *Sep. Purif. Technol.*, 51 (2006), 48–56.
- [2] Q. Liu, B.Q. Shentu, C. Gu, Z.X. Weng, The initial oxidation polymerization kinetics of 2,6-dimethylphenol with a  $\text{Cu-EDTA}$  complex in water, *Eur. Polym. J.*, 45 (2009), 1080–1085.
- [3] D. Kolodyńska, H. Hubicka, Z. Hubicki, Sorption of heavy metal ions from aqueous solutions in the presence of EDTA on monodisperse anion exchangers, *Desalination*, 227 (2008) 150–166.
- [4] S.H. Lan, F. Ju, X.W. Wu, Treatment of wastewater containing  $\text{EDTA-Cu(II)}$  using the combined process of interior microelectrolysis and Fenton oxidation-coagulation, *Sep. Purif. Technol.*, 89 (2012) 117–124.
- [5] O. Gyliene, R. Rekertas, M. Šalkauskas, Removal of free and complexed heavy-metal ions by sorbents produced from fly (*Musca domestica*) larva shells, *Water Res.*, 36 (2002) 4128–4136.
- [6] P.X. Wu, J.B. Zhou, X.R. Wang, Y.P. Dai, Z. Dang, N.W. Zhu, P. Li, J.H. Wu, Adsorption of  $\text{Cu-EDTA}$  complexes from aqueous solutions by polymeric Fe/Zr pillared montmorillonite: behaviors and mechanisms, *Desalination*, 277 (2011) 288–295.
- [7] X. Yang, J.N. Wang, C. Cheng, Preparation of new spongy adsorbent for removal of  $\text{EDTA-Cu(II)}$  and  $\text{EDTA-Ni(II)}$  from water, *Chin. Chem. Lett.*, 24 (2013) 383–385.
- [8] H.B. Zhen, Q. Xu, Y.Y. Hu, J.H. Cheng, Characteristic of heavy metals capturing agent dithiocarbamate (DTC) for treatment of ethylene diamine tetraacetic acid- $\text{Cu}$  ( $\text{EDTA-Cu}$ ) contaminated wastewater, *Chem. Eng. J.*, 209 (2012) 547–557.
- [9] C. Chang, Y. Ku, The adsorption and desorption characteristics of  $\text{EDTA}$ -chelated copper ion by activated carbon, *Sep. Sci. Technol.*, 30 (1995), 899–915.
- [10] M. Chikhi, F. Balask, R. Benchaabi, A. Ayat, K. Maameche, A.H. Meniai, Experimental study of coupling complexation-adsorption of  $\text{Cu(II)}$  on activated carbon, *Energy Procedia*, 6 (2011) 284–291.
- [11] J.K. Yang, S.M. Lee, A.P. Davis, Effect of background electrolytes and pH on the adsorption of  $\text{Cu(II)/EDTA}$  onto  $\text{TiO}_2$ , *J. Colloid Interface Sci.*, 295 (2006) 14–20.
- [12] F. Ju, Y.Y. Hu, J.H. Cheng, Removal of chelated  $\text{Cu(II)}$  from aqueous solution by adsorption-coprecipitation with iron hydroxides prepared from microelectrolysis process, *Desalination*, 274 (2011) 130–135.
- [13] R. Kumar, M.A. Barakat, Y.A. Daza, H.L. Woodcock, J.N. Kuhn,  $\text{EDTA}$  functionalized silica for removal of  $\text{Cu(II)}$ ,  $\text{Zn(II)}$  and  $\text{Ni(II)}$  from aqueous solution. *J. Colloid Interface Sci.*, 408 (2013) 200–205.
- [14] Y.X. Zhang, X.D. Hao, F. Li, Z.P. Diao, Z.Y. Guo, J. Li, pH-dependent degradation of methylene blue via rational-designed  $\text{MnO}_2$  nanosheet-decorated diatomites, *Ind. Eng. Chem. Res.*, 53 (2014) 6966–6977.

- [15] R. Ballesteros, D.P. Quintanilla, M. Fajardo, I.D. Hierro, I. Sierra, Adsorption of heavy metals by pyrimidine-derived mesoporous hybrid material, *J. Porous. Mater.*, 17 (2010) 417–424.
- [16] A.K. Johnson, J. Kaczor, H.M. Han, M. Kaur, G.X. Tian, L.F. Rao, Y. Qiang, A.J. Paszczynski, Highly hydrated poly(allylamine)/silica magnetic resin, *J. Nanopart. Res.*, 13 (2011) 4881–4895.
- [17] J.W. Choi, S.Y. Lee, S.H. Lee, K.B. Lee, D.J. Kim, S.W. Hong, Adsorption of phosphate by amino-functionalized and co-condensed SBA-15. *Water Air Soil Pollut.*, 223 (2012) 2551–2562.
- [18] M. Mureseanu, V. Părvulescu, R. Ene, N. Cioateră, T.D. Pasatoiu, M. Andruh, Cu(II) complexes immobilized on functionalized mesoporous silica as catalysts for biomimetic oxidations, *J. Mater. Sci.*, 44 (2009) 6795–6804.
- [19] L.Y. Wu, H.J. Wang, H.C. Lan, H.J. Liu, J.H. Qu, Adsorption of Cu(II)-EDTA chelates on tri-amino-functionalized mesoporous silica from aqueous solution, *Sep. Purif. Technol.*, 117 (2013) 118–123.
- [20] H. Zhang, M. Xu, H.J. Wang, D. Lei, D. Qu, Y.J. Zhai, Adsorption of copper by aminopropyl functionalized mesoporous delta manganese dioxide from aqueous solution, *Colloids Surf., A*, 435 (2013) 78–84.
- [21] R.S. Juang, C.Y. Ju, Equilibrium sorption of copper(II)-ethylenediaminetetraacetic acid chelates onto cross-linked, polyaminated chitosan beads, *Ind. Eng. Chem. Res.*, 36 (1997) 5403–5409.
- [22] W. Maketon, C.Z. Zenner, K.L. Ogden, Removal efficiency and binding mechanisms of copper and copper-EDTA complexes using polyethyleneimine, *Environ. Sci. Technol.*, 42 (2008) 2124–2129.
- [23] K.F. Hayes, C. Papelis, J.O. Leckie, Modeling ionic strength effects on anion adsorption at hydrous oxide/solution interfaces, *J. Colloid. Interface Sci.*, 125 (1998), 717–726.
- [24] A.S.M. Chong, X.S. Zhao, Functionalization of SBA-15 with APTES and characterization of functionalized materials, *J. Phys. Chem. B*, 107 (2003), 12650–12657.
- [25] X.P. Dong, W.H. Shen, Y.F. Zhu, L.M. Xiong, J.L. Shi, Facile synthesis of manganese-loaded mesoporous silica materials by direct reaction between  $\text{KMnO}_4$  and an in-situ surface template, *Adv. Funct. Mater.*, 15 (2005), 955–960.
- [26] R. Han, W.H. Zou, Z.P. Zhang, J. Shi, J.J. Yang, Removal of copper(II) and lead(II) from aqueous solution by manganese oxide coated sand I. Characterization and kinetic study, *J. Hazard. Mater.*, 137 (2006), 384–395.
- [27] J.A. Bae, S.H. Hwang, K.C. Song, J.K. Jeon, Y.S. Ko, J.H. Yim, Synthesis of functionalized mesoporous materials with various organo-silanes, *J. Nanosci. Nanotechnol.*, 10 (2010), 290–296.
- [28] M.V. Lombardo, M. Videla, A. Calvo, F.G. Requejo, G.J.A.A. Soler-Illia, Aminopropyl-modified mesoporous silica SBA-15 as recovery agents of Cu(II)-sulfate solutions: adsorption efficiency, functional stability and reusability aspects, *J. Hazard. Mater.*, 223–224 (2012), 53–62.